

Simulations and Optimization of Manufacturing of Automotive Parts

Lukasz Rauch, Monika Pernach, Jan Kusiak and Maciej Pietrzyk
AGH University of Science and Technology, al. Mickiewicza 30, 30-059, Krakow, Poland

Keywords: Computing Costs, DP Steels, Simulation of Manufacturing, Car Body Part.

Abstract: Fast progress in modeling of metal processing encourage researchers to look for better technologies, which can be done through optimization of their design. Authors have developed the computer system *ManuOpti* for optimization of manufacturing chains based on materials processing. Application of this system to simulations and optimization of manufacturing of automotive parts was the general objective of the paper. *ManuOpti* software enables performing optimization by the user with little experience in the computer science and in the optimization methods. On the other hand, the application of the optimization techniques is efficient only when reliable material models and accurate numerical methods are applied. Therefore, validation of models describing microstructure evolution in automotive steel (Dual Phase – DP) was the next objective of the paper. Physical simulations of thermal cycles were performed and the experimental results were used to validate the model. Numerical tests with the *ManuOpti* system recapitulate the paper. Case studies for the tests included various thermal cycles of the continuous annealing of DP steels.

1 INTRODUCTION

Fast progress in modeling of metal processing is observed and multi physics models are commonly applied in simulation of material behavior. Combined thermal-mechanical-thermodynamic models are used to account directly for the microstructural features of the material, as it is shown schematically in Figure 1. Prediction of micro-structure and properties of products became an inseparable part of simulations and these parameters are often used in objective functions in optimization of metal forming processes.

All these discussed aspects of modeling involve long computing times when applied to industrial forming processes, in particular when FE model is

used in connection with the optimization task. Further increase of the computing costs is observed when the whole manufacturing chains are to be optimized. It often makes industrial applications of this approach impossible. Therefore, the objective of Authors' research has been for some time focused on making simulation and optimization of metal forming processes more efficient and user friendly (Rauch et al., 2014a; Kusiak et al., 2015). The computer system *ManuOpti* for optimization of manufacturing chains was developed (Rauch, 2014b). *ManuOpti* is the software responsible for flexible integration of various external computer programs for numerical simulations, libraries of optimization methods, sensitivity analysis, metamodels and material databases. Graphical User Interface (GUI) is an important part of the *ManuOpti*, which enables working with this system for the user with little experience in the computer science and in the optimization methods

The particular objectives of this work were twofold. The first was validation of models applied to simulations of manufacturing of automotive part. This part of the paper recapitulates and systemizes Authors earlier research (Pietrzyk and Kuziak, 2012; Pietrzyk et al., 2014a). The second was performing numerical tests with the system *ManuOpti* and application of this system to optimization of manufacturing of the automotive part.

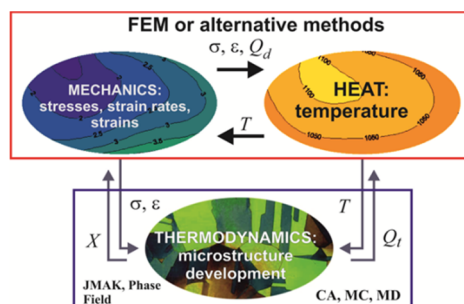


Figure 1: Multi physics model (σ - stress, ε - strain, Q_d - deformation heating, T - temperature, Q_f - heat due to phase transformations, X - volume fraction of phases.

2 MANUFACTURING OF AUTOMOTIVE PARTS

The manufacturing chain for automotive parts, which are responsible for the safety of passengers, is described briefly in this chapter. This chain will be a subject of simulation and optimization in the paper.

2.1 Advanced Steels for Automotive Parts

There has been an enormous progress made in development of materials for automotive industry during the last half of the century. Competition between steels and non-ferrous metals has been observed and in the case of former materials, it led to four important milestones: High Strength Low Alloyed Steels (HSLA) (1980-ies), Advanced High Strength Steels (AHSS) (1990-ies), 2nd generation AHSS (2000) and 3rd generation AHSS (2010). The last group of steels is presently investigated in many laboratories. These steels offer comparable or even improved capabilities at significantly lower cost. For more information about the family of the AHSSs see (Hofmann et al., 2005; Matloch et al., 2009).

Obtaining of specific features and properties in AHSSs is based on specific control of thermal cycles during production to obtain required multiphase microstructures. Numerical simulations of thermal-mechanical-microstructural phenomena occurring during manufacturing of these steels support design of optimal technologies. Manufacturing of a crash box made from AHSS was a subject of analysis in the present paper. Dual Phase (DP) steel was selected for this analysis. These steels are commonly used not only for vehicle body but also for controlled crashing zone components (Gronostajski et al., 2014). Essentially, two phase microstructure containing predominantly ferrite (F) and 20-30% of

martensite (M) gives unique properties of DP steels. Beyond the martensite, small amounts of bainite (B) or retained austenite (RA) can appear in the DP steels, but the total volume fraction of hard constituents (M+B+RA) should not exceed 30%. Typical DP microstructure from the scanning microscope is shown in Figure 2.

The morphology and volume fraction of martensite, as well as its chemical composition and hardness, are the main factors, which influence properties of products. In the case of the crash box the capability to accommodate the energy during collision is the most important property. This capability increases when strength, hardening coefficient and elongation in the tensile test (ductility) increase. These are usually contradictory features – increase of strength is in general connected with the decrease of ductility. This problem was partly overcome by development of multiphase steels (AHSS), which combine good strength with the ductility. It is achieved by combination of the soft ferritic matrix (ductility) with hard constituents (strength), see Figure 2. Required relation between volume fractions of ferrite and martensite, which is crucial for the quality of DP steels, is obtained by applying special cooling paths. The general idea is fast cooling of the steel to the temperature of maximum rate of the ferritic transformation, maintaining at this temperature for the time needed to obtain required volume fraction of ferrite and further fast cooling to transform the remaining austenite into hard constituents. Practical realization of this cycle is described in the next section. Modeling of metallurgical phenomena occurring in the microstructure during this cycle is the scope of this paper. The objective was to control processing parameters to obtain required microstructure.

2.2 Manufacturing Chain

The manufacturing chain for automotive parts is shown schematically in Figure 3. This chain includes hot strip rolling, laminar cooling, continuous annealing, stamping and welding. Simulation and optimization includes also exploitation of products, where the in use properties are checked and can be used in the goal function in the optimization task. In the case of the crash box, which was selected for the analysis in the present paper, the exploitation means the crash tests, where capability of the product to accommodate the energy during car collision is evaluated.

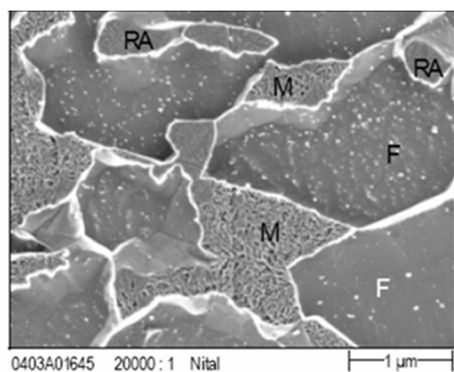


Figure 2: Typical DP microstructure.

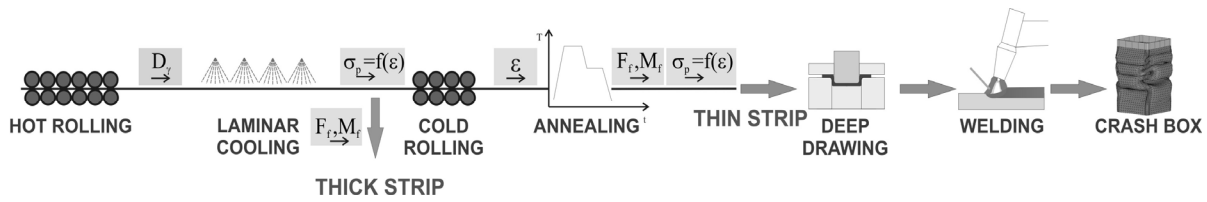


Figure 3: Manufacturing chain for automotive parts.

Two-phase microstructure can be obtained in one of the following two operations in this manufacturing cycle. The first is laminar cooling, in which thicker strips made of DP steels can be obtained. The second is continuous annealing after cold rolling, in which thinner DP steel strips are produced. Optimization of the laminar cooling was described by Pietrzyk et al. (2014a) and it is not considered in the present work. The focus is on the continuous annealing as a process, in which two-phase microstructure is obtained in the thinner strips.

Simulations of the whole manufacturing chain in Figure 3 were performed by the Authors, see paper by Kuziak and Pietrzyk (2011). The parameters, which are transferred between the processes in simulations, are shown in Figure 3. They include grain size D_γ after hot rolling, flow stress σ_p after laminar cooling, strain ϵ after cold rolling and volume fractions of phases F_f, F_m (ferrite, martensite) and flow stress σ_p after continuous annealing.

The objective of simulation and optimization of the manufacturing chain in Figure 3 is design of the best technology, which will give maximum capability of product to accumulate the energy of deformation. It was shown by Ambrozinski et al. (2015) that capability of energy accumulation is correlated with the volume fractions of phases in the DP steel. Therefore, the objective function in optimization was formulated as required volume fractions of ferrite and martensite. Sensitivity analysis performed by Szeliga et al. (2013) has shown that parameters of hot rolling and laminar cooling have small influence on the phase composition after continuous annealing. Moreover, cold rolling parameters are limited by the technological constraints. Thus the total reduction in the cold rolling is between 60 and 70% and in this range the influence of the reduction on the phase volume fractions after annealing is negligible. Therefore, in the present paper the results of simulations of the whole manufacturing chain are presented and optimization was constrained to the parameters of the continuous annealing process.

3 MODELS

The models, which were used to simulate the manufacturing chain for automotive parts are described in this section. For each process in Figure 3 models of various complexities were developed by the Authors. The models ranged from simple closed form equations describing selected parameters to advanced multiscale approaches combining FE code in macro scale with the Cellular Automata method in micro scale, see for example (Pietrzyk et al., 2014b). Selection of the best model of each process in the cycle for the purpose of the optimization of the manufacturing technology is described in (Rauch et al., 2014a). All these models are discussed below

3.1 Hot and Cold Rolling

Metamodel trained on the basis of FE simulations was used to calculate forces in hot rolling. Temperatures in this process were calculated using 1D FE solution of the heat transfer equation through the strip thickness. Microstructure evolution was described by closed form equations based on fundamental works of Sellars (1979), which were implemented in the 1D FE code. See (Kuziak and Pietrzyk, 2011) for more details on modeling of the hot strip rolling. Cold rolling process, which was not included into optimization, was simulated using 2D FE program described by Pietrzyk (2000).

Identification of coefficients in the models was essential for the accuracy of the simulations. The coefficients were identified on the basis of compression tests (flow stress) and stress relaxation tests (microstructure evolution). Various steels were investigated in the project but all the results in the present paper were obtained for the DP600 steel containing 0.09%C, 1.42%Mn, 0.1%Si, 0.35%Cr and 0.053%Al. Identification of the coefficients in the flow stress model was performed using the Authors' inverse algorithm (Szeliga et al., 2006) for the uniaxial compression tests, which were performed on the Gleeble 3800 in the Institute for

Ferrous Metallurgy in Gliwice, Poland. Flow stress equations for hot and cold rolling have the form:

$$\sigma_h = 3255 \varepsilon^{0.2} e^{-0.28\varepsilon} \dot{\varepsilon}^{0.12} e^{-0.003T} \quad (1)$$

$$\sigma_c = 908.2 \varepsilon^{0.137} \dot{\varepsilon}^{0.0019} \quad (2)$$

where: σ_h , σ_c - flow stress in hot and cold rolling, respectively, in MPa, ε - strain, $\dot{\varepsilon}$ - strain rate in s^{-1} , T - temperature in $^{\circ}C$.

3.2 Phase Transformations

Five transformations may occur during laminar cooling and continuous annealing processes. Four of them are diffusive transformations. Ferritic-pearlitic microstructure is transformed into austenite during heating. During cooling austenite is transformed into ferrite, pearlite, bainite and into martensite. The last transformation does not involve long range diffusion. Model of diffusive phase transformations was based on the JMAK (Johnson, Mehl, Avrami, Kolmogorov) equation:

$$X = 1 - \exp(-kt^n) \quad (3)$$

where: k , n - coefficients, t - time in seconds???

The model for all transformations contains 26 coefficients, which are grouped in the vector \mathbf{a} . Upgrade of the JMAK equation (3) used in the present work is described by Kuziak and Pietrzyk (2012). Briefly, constant value of the coefficient n was assumed and this coefficient is represented by a_6 , a_7 , a_{16} and a_{24} for austenitic, ferritic, pearlitic and bainitic transformations, respectively. Coefficient k was introduced as function of the temperature and the following functions were used for austenitic (k_a), ferritic (k_f) and bainitic (k_b) transformations:

$$k_a = a_1 \exp\left[\frac{a_2}{R(T+273)}\right] \quad (4)$$

$$k_f = \frac{a_8}{D_\gamma} \exp\left\{-\left[\frac{T - \left(A_{c3} + \frac{400}{D_\gamma} - a_9\right)}{a_{10}}\right]^{a_{11}}\right\} \quad (5)$$

$$k_b = a_{26} \exp(a_{25} - 0.01a_{24}T) \quad (6)$$

where: R - gas constant.

Constant value of the coefficient $k_p = a_{15}$ was assumed for the pearlitic transformation. Incubation time has to be introduced before austenitic (τ_a), pearlitic (τ_p) and bainitic (τ_b) transformations and the following equations were used:

$$\tau_a = \frac{a_4}{(T - A_{c1})^{a_6}} \exp\left[\frac{a_5}{R(T+273)}\right] \quad (7)$$

$$\tau_p = \frac{a_{12}}{(A_{c1} - T)^{a_{14}}} \exp\left[\frac{a_{13}}{R(T+273)}\right] \quad (8)$$

$$\tau_b = \frac{a_{17}}{(a_{20} - T)^{a_{19}}} \exp\left[\frac{a_{18}}{R(T+273)}\right] \quad (9)$$

The remaining equations in the model were:

$$B_s = a_{20} - 425[C] - 42.5[Mn] - 31.5[Ni] \quad (10)$$

$$M_s = a_{25} - a_{26}C_\gamma \quad (11)$$

$$F_m = \zeta \left\{1 - \exp[-0.011(M_s - T)]\right\} \quad (12)$$

where: $\zeta = 1 - (F_f + F_p + F_b)$, B_s , M_s - start temperatures for bainitic and martensitic transformation, respectively, in $^{\circ}C$, F_f , F_p , F_b , F_m - volume fraction of ferrite, pearlite, bainite and martensite, respectively.

Coefficients in equations (4) - (12) obtained by the inverse analysis of dilatometric tests for the investigated steel are given in Table 1. The phase transformations model with optimized coefficients was used in the present paper for simulation and optimization of the continuous annealing with the phase composition used in the objective function.

3.3 Model Validation

Good reliability and accuracy of the hot and cold rolling processes was confirmed in (Kuziak and Pietrzyk, 2011; Madej et al, 2015). Since the final product properties are obtained either during laminar cooling or during continuous annealing, validation of the phase transformation model during these

Table 1: Coefficients in the phase transformations model obtained by the inverse analysis of dilatometric tests for the investigated steel DP600.

a_1	a_2	a_3	a_4	a_5	a_6	a_7	a_8	a_9	a_{10}	a_{11}	a_{12}	a_{13}
32774	8.53	2.88	9.5×10^9	229.3	1.21	1.48	7.1	145.9	36.8	2.09	1397	67.7
a_{14}	a_{15}	a_{16}	a_{17}	a_{18}	a_{19}	a_{20}	a_{21}	a_{22}	a_{23}	a_{24}	a_{25}	a_{26}
3.47	0.127	1.86	24.2	24.9	1.7	683.3	0.006	0.187	0.518	0.462	428	2.9

processes is essential. The former process was thoroughly investigated by Pietrzyk et al. (2014b), therefore, in the present paper the focus was on the continuous annealing. Physical simulations of thermal cycles characteristic for the continuous annealing were performed on the dilatometer according to the general scheme shown in Figure 4.

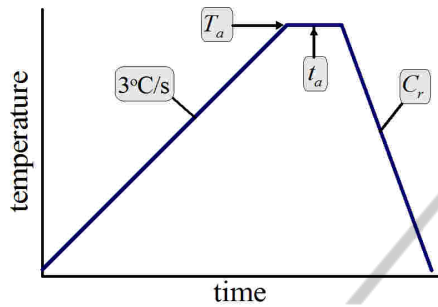


Figure 4: Thermal cycles used in the experiments.

All the tests were performed at the Institute for Ferrous Metallurgy in Gliwice, Poland. The samples were heated to the temperature T_a with the heating rate of 3°C/s , maintained at that temperature for the time t_a and cooled with various cooling rates C_r . The following values of parameters were used in the experiments: temperatures $T_a = 790^\circ\text{C}$, 830°C and 920°C ; times $t_a = 0$ s and 20 s; cooling rates $C_r = 1, 5, 10, 20, 40$ and 300°C/s . More details about these experiments can be found in (Gorecki et al., 2015).

Temperatures T_a were selected that way that 790°C was in the intercritical region (between A_{c1} and A_{c3}) and two phases ferrite and austenite were in the microstructure, 830°C was equal to A_{c3} for the considered steel and 920°C was in the austenitic region. Start and end temperatures of transformations were measured. Microstructure of each sample after the test was investigated and volume fractions of phases were evaluated, although this measurement was very difficult and obtained values could be considered as estimation only. Simulations of all experimental thermal cycles were performed and the results were compared. Selected results only are presented in the following figures.

Comparison of the start and end temperatures for the sample heated to 920°C and cooled with various rates is shown in Figure 5. Comparison of the measured and calculated volume fraction of the austenite in the microstructure gave the following results. $F_a = 15, 60$ and 100% from measurements and $F_a = 14.1, 58.3$ and 100% from calculations, for $T_a = 790^\circ\text{C}$, 830°C and 920°C , respectively.

Further validation involved comparison of measured and predicted volume fractions of phases.

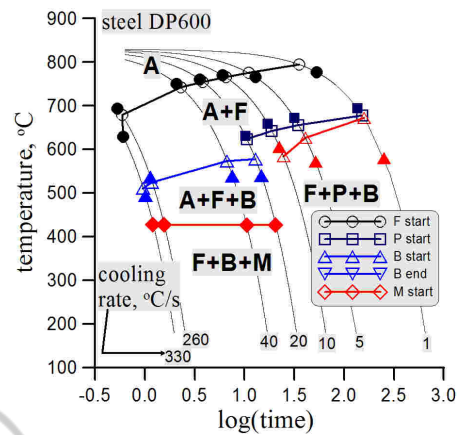


Figure 5: Comparison of the measured (full symbols) and calculated (open symbols with lines) start and end temperatures for the sample heated to 920°C and cooled with various rates.

However, as it has already been mentioned, distinguishing the phases in the experimental samples was difficult. Therefore, comparison was limited to soft (ferrite + pearlite) and hard (bainite + martensite) constituents. Selected results of the comparison are shown in Figure 6. On the basis of earlier research (Kuziak and Pietrzyk, 2011) and on the basis of models validation, it can be concluded that the models predict with good accuracy forces, temperatures and austenite grain size during rolling, as well as kinetics of phase transformations during laminar cooling and continuous annealing. The models were used for simulations of the manufacturing chain for the automotive part and the results are presented in the next section.

4 SIMULATION OF THE MANUFACTURING CHAIN

Simulations of the whole manufacturing chain presented in Figure 3 were performed and the results are presented below. 6 stand hot strip rolling mill was considered. Slab cross section was 40.6×1500 mm and the final strip thickness was 3.4 mm. Rolling schedule was $40.6 \rightarrow 21.3 \rightarrow 11.4 \rightarrow 7.0 \rightarrow 4.9 \rightarrow 4.0 \rightarrow 3.4$ mm and strip velocities at the exit from subsequent stands were 0.83, 1.6, 2.98, 4.86, 6.94, 8.5 and 9.7 mm/s. Figure 7 shows calculated forces, temperatures at two locations and austenite grain size during rolling. Comparison of forces and temperatures with measurements confirmed again good predictive capabilities of the models.

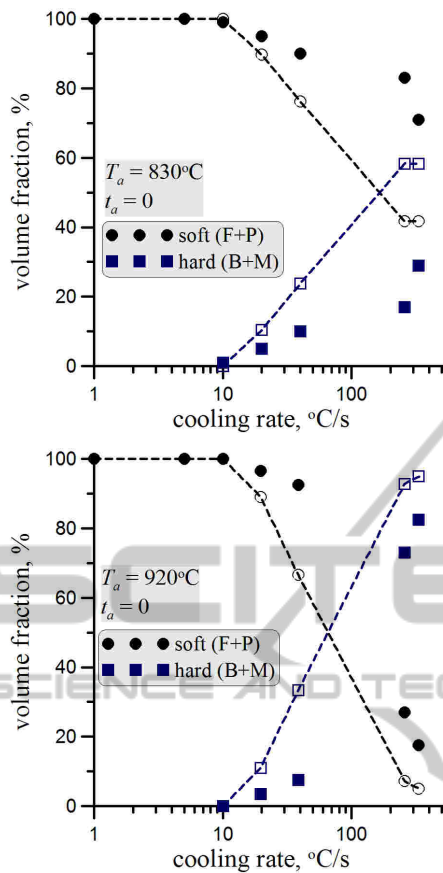


Figure 6: Comparison of the measured (full symbols) and calculated (open symbols with lines) soft (ferrite + pearlite) and hard (bainite + martensite) constituents.

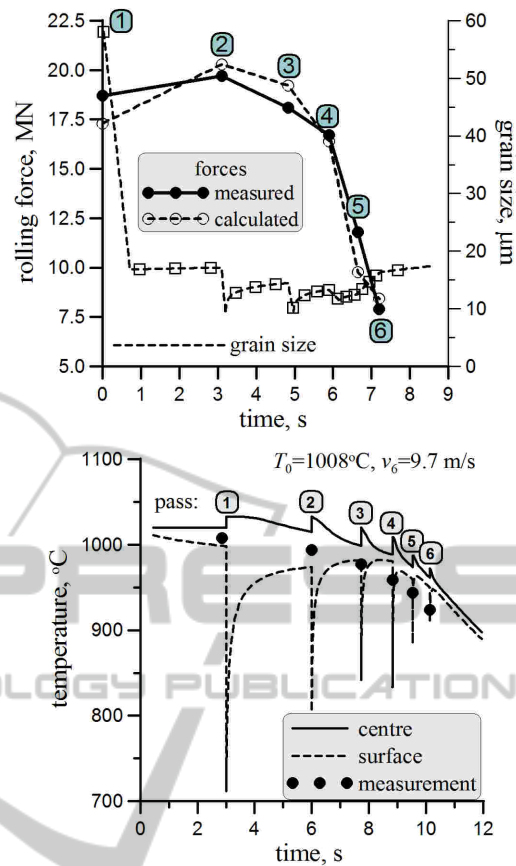


Figure 7: Comparison of the measured (full symbols) and calculated (open symbols with lines) soft (ferrite + pearlite) and hard (bainite + martensite) constituents.

Laminar cooling and cold rolling were simulated next. Full results of these simulations are given in (Pietrzyk et al., 2014a) and in (Madej et al., 2015) for laminar cooling and cold rolling, respectively. These results are not repeated in the present paper. The main focus was put on simulations of the continuous annealing. Typical thermal cycle for this process is shown in Figure 8. In this figure t represents time, H_r represents heating rate and C_r cooling rate. During heating the recrystallization of the ferrite occurs first and it is followed by austenitic transformation. Depending on the maximum temperature of the cycle (T_a) the process is classified as intercritical ($A_{c1} < T_a < A_{c3}$) or fully austenitized ($T_a > A_{c3}$).

Results of simulations for two temperatures T_a (810°C and 850°C) are presented below. Heating rate H_{r1} was 10°C/s, in the second stage $t_{h2} = 40$ s and $H_{r2} = 0.25$ °C/s. Time t_{c2} was the second varying parameter and values 4 and 8 s were considered.

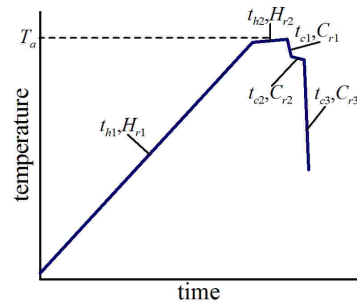


Figure 8: Typical continuous annealing thermal cycle.

Remaining parameters were $C_{r1} = 60$ °C/s, $C_{r3} = 100$ °C/s, $C_{r2} = 1.5$ °C/s. Calculated changes of the ferrite volume fraction during four investigated cycles of the continuous annealing are shown in Figure 9 (A: $T_a = 810$ °C, $t_{c2} = 4$ s; B: $T_a = 810$ °C, $t_{c2} = 8$ s; C: $T_a = 850$ °C, $t_{c2} = 4$ s; D: $T_a = 850$ °C, $t_{c2} = 8$ s;). Calculated volume fractions of ferrite after heating ("old" ferrite) and volume fraction of ferrite and martensite after four investigated cycles of the continuous annealing are shown in Figure 10.

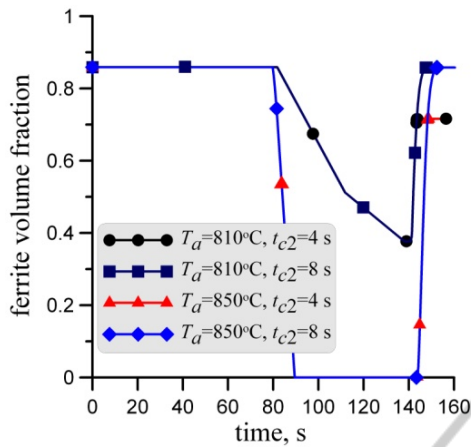


Figure 9: Changes of the ferrite volume fraction during four investigated cycles of the continuous annealing.

Microstructure after annealing was accounted for in the material model for simulations of the stamping process and the crash test. Calculated stresses and strains for the two steps of stamping of the crash box are shown in Figure 11. Results of simulation of the crash test with strain distributions are shown in Figure 12. The original crash box with stains transformed from the stamping, as well as the crash box after the test, are shown in this figure.

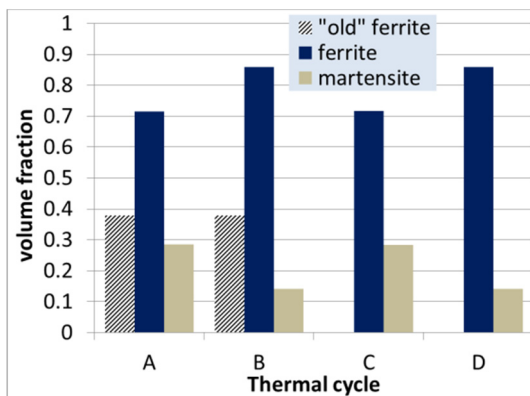


Figure 10: Calculated volume fraction of ferrite after heating ("old" ferrite) and volume fractions of ferrite and martensite after investigated cycles of the annealing.

All results presented in this section of the paper, as well as in publications (Kuziak and Pietrzyk, 2011) for hot rolling, (Pietrzyk et al., 2014b) for laminar cooling and (Ambrozinski et al., 2015) for stamping and crash tests, confirmed capabilities of the models to simulate the whole manufacturing chain for automotive parts.

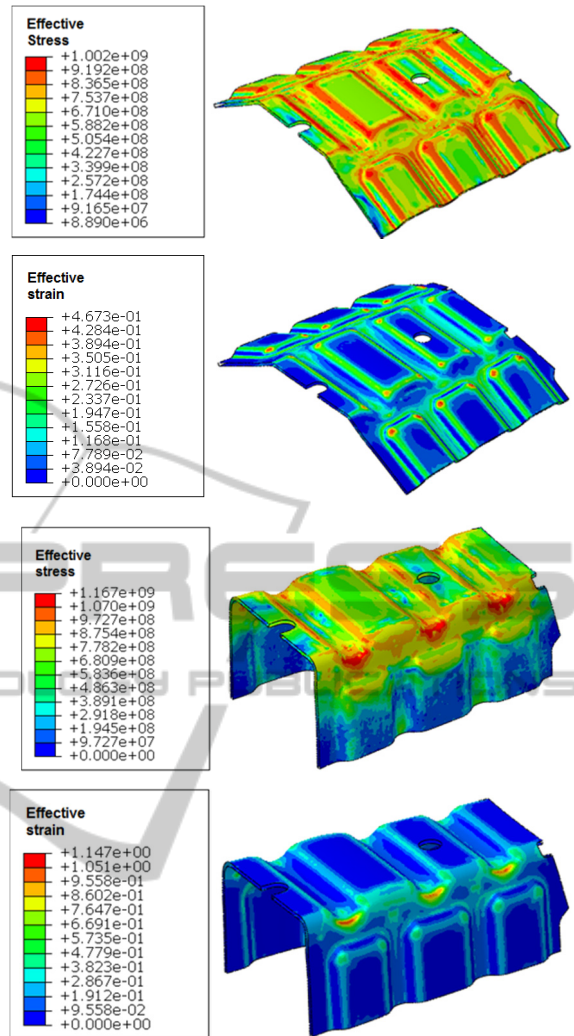


Figure 11: Calculated effective stress and effective strain for the step 1 (top) and step 2 (bottom) during stamping of the crash box (Ambrozinski et al., 2015).

5 OPTIMIZATION OF THE CONTINUOUS ANNEALING

Models described in section 3 were implemented in the *ManuOpti* system for optimization of manufacturing chain. Details of the computer science basis of the system are given by Rauch et al. (2014b) and examples of its various applications are described by Kuziak et al. (2015). In the developed system the functionality of optimization is covered by numerical modules, which can be directly imported into the system in a form of dynamically linked libraries (*dll* files). The main requirement is that each library has to possess the class called *Main*, which supports listing of available

optimization tools and their parameters through the listing method. Besides this functionality, the system is equipped with built in library with conventional optimization methods, as well as nature inspired algorithms. Additionally, the optimization strategy, which allows selection and configuration of the best method for the analyzed problem is equipped with the library.



Figure 12: Strain distribution in the crash box before and after deformation (Ambrozinski et al., 2015).

6 OPTIMIZATION OF THE CONTINUOUS ANNEALING

Models described in section 3 were implemented in the *ManuOpti* system for optimization of manufacturing chain. Details of the computer science basis of the system are given by Rauch et al. (2014b) and examples of its various applications are described by Kusiak et al. (2015). In the developed system the functionality of optimization is covered by numerical modules, which can be directly imported into the system in a form of dynamically linked libraries (*dll* files). The main requirement is that each library has to possess the class called *Main*, which supports listing of available optimization tools and their parameters through the listing method. Besides this functionality, the system is equipped with built in library with conventional optimization methods, as well as nature inspired algorithms. Additionally, the optimization strategy, which allows selection and configuration of the best method for the analyzed problem is equipped with the library.

Graphical User Interface (GUI) is an important part of the system, which enables working with this system for the user with little experience in the computer science and in the optimization methods. To facilitate creation and parameterization of production cycles through the GUI, the system gathers information about single processes, which

can be flexibly joined together by using specially prepared converters. The system communicates with FE commercial software, as well as with in-house software used in production optimization.

Computer system *ManuOpti* was applied to optimization of the continuous annealing. The objective of the optimization was to obtain 20% of martensite and as low as possible volume fraction of bainite in the microstructure, with 40% of the intercritical ferrite. The objective function was formulated as follows:

$$\Phi = \sqrt{w_1 (F_m - F_{m0})^2 + w_2 F_b^2 + w_3 (F_{if} - F_{if0})^2} \quad (13)$$

where: w_1, w_2 – weights, F_{if} – volume fraction of the intercritical ferrite, respectively, F_{m0}, F_{if0} – required volume fraction of martensite and intercritical ferrite, respectively.

Parameters of the thermal cycle shown in Figure 8 were the design variables. Optimization of the objective function (13) gave the thermal cycle shown by the dashed line in Figure 13. Continuous lines in this figure represent changes volume fractions of phases during this cycle. It is seen that required volume fractions of phases were obtained.

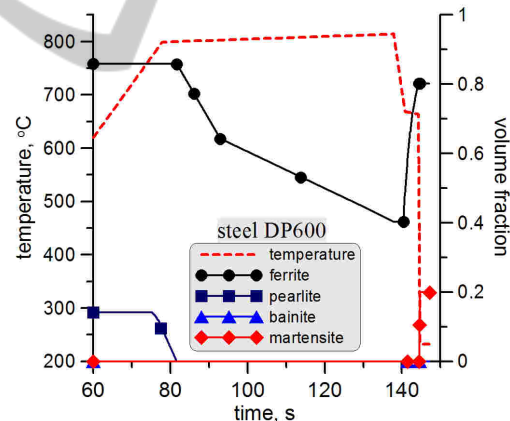


Figure 13: Optimal thermal cycle of the continuous annealing (dotted line) and kinetics of transformations during this cycle.

7 SUMMARY

Simulation of the manufacturing cycle for automotive parts was presented in the paper. Analysis of results has shown that the final properties of product are obtained in the continuous annealing and this process was selected for the optimization. Computer system supporting design of

production processes and cycles in metal forming industry was used. The system is user friendly and adapts easily to new use cases. Performed optimization allowed to design the thermal cycle, which gives required volume fraction of phases in the final product.

ACKNOWLEDGEMENTS

Financial assistance of the NCN, project no. 2011/03/B/ST8/06100, is acknowledged.

REFERENCES

- Ambroziński, M., Polak, S., Gronostajski, Z., Kuziak, R., Chorzępa, W., Pietrzyk, M., 2015, Numeryczna symulacja testu zderzeniowego z uwzględnieniem umocnienia odkształceniowego w procesie wytwarzania energochłonnego elementu samochodu (Numerical simulation of the crash test accounting for strain hardening introduced during the manufacturing stage), *Mechanik*, 88, 92-96 (in Polish).
- Górecki G., Kuziak R., Kwiaton N., Madej Ł., Pietrzyk M., 2015, DP_builder - the computer system for the design of the continuous annealing cycles for DP steels, *Computer Methods in Materials Science*, 14, (in press).
- Gronostajski, Z., Niechajowicz, A., Polak, S., 2010. Prospects for the use of new generation steel of the AHSS type for collision energy absorbing components, *Archives of Metallurgy and Materials*, 55, 221-230.
- Hofmann, H., Mattissen, D., Schaumann, T.W., 2009. Advanced cold rolled steels for automotive applications, *Steel Research International*, 80, 22-28.
- Kuziak, J., Rauch, Ł., Pietrzyk, M., 2015. Holistic approach to optimal design of technology of materials processing, *Proc. XXXIV Verformungskundliches Kolloquium*, ed., Buchmayr, B., Zauchensee, 56-66.
- Kuziak, R., Pietrzyk, M., 2011, Physical and numerical simulation of the manufacturing chain for the DP steel strips, *Steel Research International, special edition Conf. ICTP, Aachen*, 756-761.
- Madej Ł., Kuziak R., Mroczkowski M., Perzynski K., Libura W., Pietrzyk M., 2015, Development of the multi scale model of cold rolling based on physical and numerical investigation of ferritic-pearlitic steels, *Archives of Civil and Mechanical Engineering*, 15, doi.org/10.1016/j.acme.2015.02.010.
- Matlock, D.K., Krauss, G., Speer, J.G., 2005. New microalloyed steel applications for the automotive sector, *Materials Science Forum*, 500-501, 87-96.
- Pietrzyk, M., Kuziak, R., 2012. Modelling phase transformations in steel, in: *Microstructure evolution in metal forming processes*, eds, Lin, J., Balint, D., Pietrzyk, M., Woodhead Publishing, Oxford, 145-179.
- Pietrzyk, M., Kuziak, R., Radwański, K., Szeliga, D., 2014a. Physical and numerical simulation of the continuous annealing of DP steel strips, *Steel Research International*, 85, 99-111.
- Pietrzyk M., Kuziak J., Kuziak R., Madej Ł., Szeliga D., Gołąb R., 2014b. Conventional and multiscale modelling of microstructure evolution during laminar cooling of DP steel strips, *Metallurgical and Materials Transactions B*, 46B, 497-506.
- Rauch, Ł., Kuziak, R., Pietrzyk, M., 2014a. From high accuracy to high efficiency in simulations of processing of Dual-Phase steels, *Metallurgical and Materials Transactions B*, 45B, 497-506.
- Rauch, Ł., Skiba, M., Kuziak, J., 2014b. Computer system dedicated to optimization of production processes and cycles in metal forming industry, *Computer Methods in Materials Science*, 14, 3-12.
- Sellars, C.M., 1979, Physical metallurgy of hot working. In *Hot working and forming processes*, eds, Sellars C.M., Davies G.J., The Metals Soc., London, 3-15.
- Szeliga, D., Gawąd, J., Pietrzyk, M., Inverse analysis for identification of rheological and friction models in metal forming, *Computer Methods in Applied Mechanics and Engineering*, 195, 2006, 6778-6798.
- Szeliga, D., Sztangret, Ł., Kuziak, J., Pietrzyk, M., 2013. Optimization as a support for design of hot rolling technology of dual phase steel strips, *Proc. 11th Conf. NUMIFORM*, AIP Publishing, Shenyang, 718-724.